HHS Public Access

Author manuscript

Mol Cancer Res. Author manuscript; available in PMC 2024 August 01.

Published in final edited form as:

Mol Cancer Res. 2024 February 01; 22(2): 209–220. doi:10.1158/1541-7786.MCR-23-0290.

SOX10 loss sensitizes melanoma cells to cytokine-mediated inflammatory cell death

Sheera R. Rosenbaum[1,#], **Signe Caksa**[1,#], **Casey D. Stefanski**[1], **Isabella V. Trachtenberg**[1], **Haley P. Wilson**[1], **Nicole A. Wilski**[1], **Connor A. Ott**[1], **Timothy J. Purwin**[1], **Jelan I. Haj**[1], **Danielle Pomante**[1], **Daniel Kotas**[1], **Inna Chervoneva**[1,2], **Claudia Capparelli**[3,4], **Andrew E. Aplin**[1,4,*]

[1]Department of Pharmacology, Physiology, and Cancer Biology, Thomas Jefferson University, Philadelphia, PA 19107, USA.

[2]Division of Biostatistics, Thomas Jefferson University, Philadelphia, PA 19107, USA.

[3]Department of Medical Oncology, Thomas Jefferson University, Philadelphia, PA 19107, USA.

[4]Sidney Kimmel Cancer Center, Thomas Jefferson University, Philadelphia, PA 19107, USA.

Abstract

The transcription factor, SOX10, plays an important role in the differentiation of neural crest precursors to the melanocytic lineage. Malignant transformation of melanocytes leads to the development of melanoma, and SOX10 promotes melanoma cell proliferation and tumor formation. SOX10 expression in melanomas is heterogeneous, and loss of SOX10 causes a phenotypic switch towards an invasive, mesenchymal-like cell state and therapy resistance; hence, strategies to target SOX10-deficient cells are an active area of investigation. The impact of cell state and SOX10 expression on anti-tumor immunity is not well understood but will likely have important implications for immunotherapeutic interventions. To this end, we tested whether SOX10 status affects the response to CD8+ T cell-mediated killing and T cell-secreted cytokines, TNFα and IFNγ, which are critical effectors in the cytotoxic killing of cancer cells. We observed that genetic ablation of SOX10 rendered melanoma cells more sensitive to CD8+ T cell-mediated killing and cell death induction by either TNFα or IFNγ. Cytokine-mediated cell death in SOX10-deficient cells was associated with features of caspase-dependent pyroptosis, an inflammatory form of cell death that has the potential to increase immune responses.

Implications: These data support a role for SOX10 expression altering the response to T cell-mediated cell death and contribute to a broader understanding of the interaction between immune cells and melanoma cells.

[*]**Corresponding author**: Andrew E. Aplin, Department of Pharmacology, Physiology, and Cancer Biology, Thomas Jefferson University, 233 South 10th Street, Philadelphia, PA 19107, USA. Tel: (215) 503-7296. Fax: (215) 923-9248; Andrew.Aplin@Jefferson.edu.

[#]These authors contributed equally to this work.

Conflict of Interest: A.E. Aplin has ownership interest in patent number 9880150 and has a pending patent, PCT/US22/76492. No potential conflicts of interest were declared by the other authors.

Keywords

SOX10; melanoma; pyroptosis; TNFα; IFNγ

Introduction

During embryonic development, the transcription factor SRY-box transcription factor 10 (SOX10) plays an essential role in the differentiation of melanocytes from the neural crest lineage (1). Transformation of melanocytes can give rise to melanoma in the skin, eye, mucosal membranes and acral sites. In cutaneous melanoma, SOX10 promotes cancer cell proliferation *in vitro* and tumor formation *in vivo* (2,3). Tumorigenesis critically relies on the development of evasion mechanisms to escape immune cell destruction (4), but the role of SOX10 in regulating anti-tumor immunity has not been well established. In concert with other developmental factors, SOX10 regulates a 'proliferative' cell state. Melanoma displays intratumoral heterogeneity and plasticity, and the loss of SOX10 expression is associated with dedifferentiation to a mesenchymal-like, invasive cell state, marked by alterations in epithelial-to-mesenchymal transition (EMT) and cell cycle signatures (5-7). The SOX10-negative cell state has also been shown to promote resistance to targeted therapy (5,7-9), but how to specifically target this resistant population remains an open question.

Anti-tumor immune responses rely on the activation of cytotoxic T cells, which can kill cancer cells through the release of cytolytic granules such as granzyme and perforin, engagement of cell death receptors, or secretion of the cytokines TNFα and IFNγ (10-12). CRISPR/Cas9-based screens have identified TNFα and IFNγ signaling pathways as critical regulators of cancer cell sensitivity to T cell cytotoxic killing and immunotherapy (13-17). Importantly, TNFα blockade reduced the ability of antigen-specific T cells to control tumor growth (13,14), and a reduction in IFNγ-driven apoptosis is associated with T cell resistance (18). Thus, cancer cell sensitivity to T cell-secreted cytokines may have important implications for the efficacy of immune cell killing.

Beyond the activation of cytotoxic effectors, successful anti-tumor immune responses rely on the ability of immune cells to properly traffic and infiltrate tumors. Currently, antibodies that target immune checkpoint proteins are FDA-approved for use in melanoma, and these therapies boost anti-tumor immunity by blocking the negative signals that dampen T cell activation. Immune checkpoint inhibitors improve patient survival in melanoma; however, 40-50% of tumors do not respond to therapy (19). Tumors that do not respond to immune checkpoint blockade exhibit lower levels of immune cell infiltrates (20); thus, strategies that increase immune infiltration to the tumor site may improve response. One such strategy is to induce pyroptotic cell death, which causes the release of inflammatory cytokines (21). Pyroptosis can promote the recruitment of immune cells and amplify anti-tumor immune responses, contributing to the success of multiple cancer therapies (21,22).

The interaction between tumor cells and immune cells is complex, and approaches to promote immune cell killing of invasive cells are an active area of investigation. In melanoma, SOX10 expression decreases the percentage of CD8+ T cells in the tumor, and loss of SOX10 delays tumor growth in a CD8+ T cell-dependent manner (23,24). In

the present study, we investigated whether SOX10 status can affect melanoma response to CD8+ T cell-mediated killing. We observed that the loss of SOX10 renders melanoma cells sensitive to either TNFα or IFNγ-induced inflammatory cell death.

Materials and Methods

Cell culture

A375 cells (purchased from ATCC in 2005, RRID: CVCL_6233) and MeWo cells (donated by Dr. Barbara Bedogni in 2014, RRID: CVCL_0445) were cultured in DMEM with 10% FBS and 1% penicillin/streptomycin. 1014 cells (donated by Dr. Lionel Larue in 2018, also known as MaNRAS2, RRID: CVCL_B9UU) were cultured in Ham's F-12 with 10% FBS and 1% penicillin/streptomycin. YUMM1.1 cells (donated by Dr. Marcus Bosenberg in 2014, RRID: CVCL_JK10) were cultured in DMEM/F-12 (1:1) with 10% FBS, 1% penicillin/streptomycin, and 1% MEM non-essential amino acids. 1014 and YUMM1.1 *Sox10*-knockout cells and A375 and MeWo *SOX10*-knockout cells were generated previously (7,23). All cells were maintained in a humidified incubator at 37°C in 5% CO_2. All cell lines were tested for mycoplasma monthly using the MycoScope Kit (Genlantis; San Diego, CA). Human cell lines were authenticated by sequencing at *NRAS* and *BRAF* loci, and STR analysis was completed for A375 parental and CR.SOX10 cells (August 2020, October 2020), MeWo parental and CR.SOX10 cells (April 2019, June 2021) and YUMM1.1 parental and CR.SOX10 cells (June 2021). All cell lines matched a known and expected STR profile. 1014 cells do not have a publicly available STR authentication profile but matched (May 2021, March 2022) to a STR profile from an early passage from that line.

Inhibitors, growth factors, and cytokines

Human recombinant IFNγ, TNFα, TRAIL, FasL, IFNα2, IFNβ1, and TGFβ1 were purchased from R&D Systems (Minneapolis, MN). Mouse recombinant IFNγ, TRAIL, and FasL were purchased from R&D Systems, and mouse recombinant TNFα was purchased from Sigma-Aldrich (St. Louis, MO). Z-VAD-FMK and staurosporine (STS) were purchased from Selleck Chemicals (Houston, TX). Necrostatin-1 (Nec-1) was purchased from Cayman Chemical Company (Ann Arbor, MI).

Western blotting

Protein lysates were collected in Laemmli sample buffer, separated by SDS-PAGE, and transferred to PVDF membranes. Immunoreactivity was detected using horseradish peroxidase-conjugated secondary antibodies (CalBioTech; Spring Valley, CA or Invitrogen; Waltham, MA) and chemiluminescence substrate (ThermoScientific; Waltham, MA) on a Versadoc or Chemidoc Imaging System (Bio-Rad; Hercules, CA). Primary antibodies are listed in Supplementary Materials and Methods. For analysis of cell supernatant, cells were plated in three wells of a 6-well plate per condition with 2 mL serum-free media −/+ cytokine treatment for 24 hours. Medium (6 mL) was collected and concentrated in Amicon Ultra-15 Centrifugal Filter tubes (EMD Millipore; Burlington, MA) to a volume of 250 μl. 15 μl of concentrate was combined with 5 μl 2X Laemmli sample buffer, and a 15 μl sample was loaded per well. Membranes were stained for 1 hour with Ponceau red solution

(Sigma-Aldrich) to assess protein loading prior to overnight incubation with HMGB1 antibody. For Western blot quantification, band intensity was analyzed in ImageJ (RRID: SCR_003070). The expression of cleaved-caspase-8 and cleaved-GSDME was normalized to actin expression for each replicate. The expression of HMGB1 was normalized to Ponceau red stain for each replicate. Uncropped blots are available in supplementary data.

Reverse Phase Protein Array (RPPA)

RPPA analysis was performed according to the protocol from the MD Anderson Reverse Phase Protein Array Core Facility (Houston, TX) (25). A375 and MeWo parental or *SOX10*-knockout cells were plated in 6-well plates (2.5×10^5 cells/well). The next day, cells were treated with either 50 ng/mL TNFα or 100 ng/mL IFNγ for 72 hours. Cells were then lysed in RPPA lysis buffer (1% Triton X-100, 50 mM HEPES (pH 7.4), 150 mM NaCl, 1.5 mM $MgCl_2$, 1 mM EGTA, 100 mM NaF, 10 mM Na pyrophosphate, 1 mM Na_3VO_4, 10% glycerol, and freshly added protease and phosphatase inhibitors (Roche; Basel, Switzerland)) for 20 minutes on ice. Lysates were centrifuged, supernatants containing protein were collected, and protein concentration was determined using a Bradford assay. Lysates from three independent experiments were run for RPPA analysis at the MD Anderson Reverse Phase Protein Array Core Facility. RPPA data were then used to determine changes in expression of cell death pathway proteins due to TNFα or IFNγ treatment in parental and *SOX10*-knockout cell lines. Comparisons were performed between each group by the two-sample t-test method with 1,000 permutations and assumed unequal variance. Antibodies with a p-value < 0.05 were considered significant. Statistical analyses were performed in Matlab® (v2022a, RRID: SCR_001622) using the mattest function. Apoptosis, ferroptosis and necroptosis pathway gene sets were collected from the Gene Ontology (26,27) and KEGG Pathway (28) databases. The pyroptosis gene set has been previously described (22). Briefly, the gene set was determined using http://amigo.geneontology.org/amigo/term/GO:0070269 and recommendations on cell death nomenclature (29), and the genes included were GSDMA/B/C/D/E, CASP1/2/3/4/5/8, NLRC4, IL1B, and IL18. RPPA data can be found in Supplementary Table S1.

Crystal violet staining

The same number of parental or *Sox10/SOX10*-knockout cells was plated in 12-well plates and treated with TNFα or IFNγ the next day. For experiments involving YUMM1.1 parental and *Sox10*-knockout cells, plates were coated with 0.01% poly-l-lysine (Sigma-Aldrich) prior to plating to improve cell adhesion. After 72 hours, cells were washed twice with PBS and stained with crystal violet solution (0.2% crystal violet in 10% buffered formalin). Plates were washed with water and air-dried. Wells were imaged using a Nikon Eclipse Ti inverted microscope with NIS-Elements AR 3.00 software (Nikon; Melville, NY, RRID: SCR_002776), and plate coverage was quantified using ImageJ.

Propidium iodide uptake assay

The same number of parental or *Sox10/SOX10*-knockout cells was plated in 12-well plates and treated with TNFα or IFNγ the next day. 0.5 μM propidium iodide (PI) was added to each well, and plates were placed into an IncuCyte S3 Live-Cell Imaging System (Essen BioScience; Goettingen, Germany, RRID: SCR_023147). Phase contrast and RFP Images

were acquired every 2 hours across 25 regions in each well at 10X magnification for 72 hours. The percentage of cells with PI uptake was calculated using the formula (percent red confluence/percent phase confluence) x 100. Cell morphology was examined after 72 hours of treatment, and plasma membrane swelling was identified.

Flow cytometry staining

The same number of parental or *Sox10/SOX10*-knockout cells was plated in 6-well plates and treated with TNFα or IFNγ the next day. For experiments involving YUMM1.1 parental and *Sox10*-knockout cells, plates were coated with 0.01% poly-l-lysine (Sigma-Aldrich) prior to plating to improve cell adhesion. For cell death analysis, cells were incubated in 100 μl of binding buffer (10 mM HEPES, 0.14 M sodium chloride, 2.5 mM calcium chloride), and stained with 5 μl of Annexin V-APC (BD Biosciences; San Jose, CA) and 2 μl of 1 mg/mL propidium iodide (ThermoScientific) for 25 min. For calreticulin staining, cells were incubated with calreticulin antibody (Cell Signaling Technology; Danvers, MA; #12238, RRID: AB_2688013) or a rabbit IgG control for 1 hour, followed by incubation with a rabbit-specific fluorochrome-conjugated secondary antibody for 30 mins (Molecular Probes; Eugene, OR), then fixed using the BD Cytofix/Cytoperm Kit from BD Biosciences. All samples were run on a BD Celesta or LSR II flow cytometer and analyzed using FlowJo software (BD Biosciences, RRID: SCR_008520).

In vitro T cell killing assays

Splenocytes were collected from the spleens of Pmel-17 mice (B6.Cg-Thy1a /Cy Tg(TcraTcrb)8Rest/J, purchased from Jackson Laboratory, RRID: IMSR_JAX:005023), and used fresh or frozen in CryoStor C10 Freeze Media (BioLife Solutions; Bothell, WA). Pmel-1 splenocytes were cultured in T cell media (RPMI-1640, 10% FBS, 1% penicillin/streptomycin, 0.00038% β-mercaptoethanol) at 1×10^6 cells per 2 mL with 1.0 μg/mL gp100 peptide (EGSRNQDWL; GeneMed, San Francisco, CA, or JPT Peptide Technologies, Berlin, Germany). Two days later, rIL2 (BioLegend; San Diego, CA) was added to the culture. Media and rIL2 was refreshed after three days. On day 7, T cells were used for killing assays. Cells were stained with a fluorochrome-conjugated anti-CD8α antibody (BioLegend; #100741, clone 53-6.7, RRID: AB_11124344) and analyzed by flow cytometry to confirm $CD8^+$ T cell purity. For co-culture assays, cancer cells plated in 6-well plates one day prior were pulsed with 1 nM gp100 peptide for 3 hours, washed twice, and then incubated with CD8+ T cells at varying ratios. For transwell co-culture assays, 0.4 μM transwell culture inserts were placed above cancer cells that had been plated in the lower chamber one day prior, while CD8+ T cells were added to the upper chamber with 1.0 μg/mL gp100 peptide added. After 48 hours of co-incubation, cancer cells were washed 3 times and stained with crystal violet solution (0.2% crystal violet in 10% buffered formalin). Wells were imaged using a Nikon Eclipse Ti inverted microscope with NIS-Elements AR 3.00 software (Nikon), and plate coverage was quantified using ImageJ. All studies involving animals were approved by the Institutional Animal Care and Use Committee (IACUC protocol #1052) and performed in a facility at Thomas Jefferson University accredited by the Association for the Assessment and Accreditation of Laboratory Animal Care (AAALAC).

TCGA analysis

The Cancer Genome Atlas (TCGA) SKCM RNA-sequencing (RNA-seq) V2 RSEM normalized counts data was collected from the Broad GDAC Firehose data run (doi:10.7908/C11G0KM9) (30,31). Gene Set Enrichment Analysis (GSEA) was performed using the pyroptosis gene set and the TCGA melanoma dataset in IGV (v2.15.2, RRID: SCR_011793) (Broad Institute and the Regents of the University of California).

Statistical analysis

All *in vitro* studies were conducted three independent times unless otherwise indicated; values were averaged, and representative images are shown. Bar graphs show mean + SD. Line graphs show mean ± SEM. For T cell killing assays and crystal violet growth assays, the log-transformed percentages of plate coverage were analyzed using linear mixed-effects (LME) models with fixed effects of treatment, clone, and their interaction, and random effect of biological replicate to adjust for correlation between multiple images per plate. Separate models were fitted for data from each cell line (including *Sox10/SOX10*-knockout clones). The residuals were evaluated to validate the assumptions of the models. The effects of treatment were evaluated and compared between clones and parental cell lines based on the fitted LME models. For Annexin V/PI staining following cytokine or staurosporine treatment, percent staining was analyzed using a two-way ANOVA model and Dunnett's correction for multiple comparisons. Annexin V/PI staining in experiments involving Z-VAD-FMK or Necrostatin-1 pre-treatment was analyzed using a two-way ANOVA model and Tukey's correction for multiple comparisons. For PI uptake assays, the area under the curve (AUC) was calculated for each replicate, and log-transformed AUCs were analyzed using a two-way ANOVA model and Bonferroni's correction for multiple comparisons. Statistical analyses were performed in GraphPad Prism (v.9.4.1, RRID: SCR_002798) or in R (R Foundation for Statistical Computing https://www.R-project.org/, RRID: SCR_001905). A p-value of < 0.05 was considered statistically significant. Significance is denoted by *p< 0.05, **p< 0.01, ***p< 0.001, ****p< 0.0001.

Data Availability Statement

TCGA data analyzed in this study were obtained from The Cancer Genome Atlas SKCM RNA-sequencing V2 RSEM normalized counts data collected from the Broad GDAC Firehose data run (doi:10.7908/C11G0KM9). All other data generated in this study are available within the article and its supplementary data files, or upon request from the corresponding author.

Results

Cytotoxic T cell-secreted cytokines reduce the growth of *SOX10/Sox10*-knockout cells

Sox10-knockout cells grow slower than their parental counterparts *in vivo* due, in part, to the presence of CD8+ T cells (23). Therefore, we used parental and *Sox10*-knockout *Nras* mutant mouse melanoma 1014 cells (Fig. 1A) to test whether SOX10 expression alters tumor cell response to CD8+ T cell-mediated killing (23,32). We expanded T cells from splenocytes of transgenic Pmel-1 mice (Suppl. Fig. 1A), a model in which T cells are

specific for the melanoma antigen gp100 (33). We pulsed parental and *Sox10*-knockout 1014 cells with gp100 peptide and co-cultured the cells with varying ratios of Pmel-1 CD8+ T cells for 48 hours. We then performed a crystal violet assay to determine the percent surviving cells at each T cell dilution relative to the untreated condition for each cell line (Fig. 1B, 1C). We observed that at low effector-to-tumor cell ratios (1:4, 1:8), 1014 CR.SOX10 #1.3 and CR.SOX10 #1.30 cells, but not parental cells, exhibited significantly decreased survival (Fig. 1B). 1014 CR.SOX10 #2.35 cells trended towards decreased survival at a 1:4 ratio. At a 1:1 ratio, T cells were effective at killing both parental and *Sox10*-knockout cells. As both direct and indirect methods of T cell killing exist, we also performed an indirect co-culture experiment where T cells and tumor cells were separated by a transwell insert. At a 1:8 effector to tumor cell ratio, two of the *Sox10*-knockout cell lines trended towards reduced survival compared to parental cells (Suppl. Fig 1B, 1C), indicating that an indirect killing method alone may be able to kill SOX10-deficient cells.

To determine whether cytotoxic T cell cytokines are more effective at reducing the growth of SOX10-deficient melanoma cells, we utilized parental and *Sox10*-knockout *Nras* mutant 1014 and *Braf* mutant YUMM1.1 mouse cells, as well as parental and *SOX10*-knockout *BRAF* mutant A375 and *BRAF* and *NRAS* wild type MeWo human cell lines (7,23) (Fig. 1A, Suppl. Fig. 1D). We treated parental and *Sox10/SOX10*-knockout cells with TNFα or IFNγ and examined cell viability by crystal violet staining (Fig. 1D-I, Suppl. Fig. 1E-F). We found that TNFα treatment reduced the growth of 1014, A375, and YUMM1.1 *Sox10/SOX10*-knockout cell lines, but not their parental counterparts (Fig. 1D-E, 1G-H, Suppl. Fig. 1E-F). IFNγ reduced the growth of both parental and *SOX10*-knockout A375 and MeWo cells (Fig. 1E-F, 1H-I). Conversely, TNFα had no effect in the MeWo cell lines and IFNγ did not consistently affect the growth of the 1014 and YUMM1.1 cell lines. These data suggest that SOX10 loss can reduce cell viability/growth in the presence of cytotoxic cytokines.

SOX10/Sox10-knockout sensitizes melanoma cells to cytokine-mediated cell death

T cell-secreted cytokines can induce cytotoxicity as well as decrease cell proliferation in tumor cells (10,11,34). To determine if cytokine treatment contributes to increased cell death in *Sox10/SOX10*-knockout cells, we treated parental and *Sox10/SOX10*-knockout cells with TNFα and IFNγ and assessed cell death by Annexin V and propidium iodide (PI) staining and flow cytometry (Fig. 2A-C, Suppl. Fig. 1G-H). A375 and YUMM1.1 parental cells were sensitive to cell death induction by IFNγ, while 1014 and MeWo parental cells were resistant (Fig. 2A-2C, Suppl. Fig 1H). In 1014 and A375 *Sox10*/*SOX10*-knockout cells, we observed a significant increase in cell death in response to TNFα treatment (Fig. 2A, 2B). YUMM1.1 *Sox10*-knockout cells trended towards increased cell death in response to TNFα treatment (Suppl. Fig 1H). We observed a significant increase in cell death in response to IFNγ, but not TNFα, in the MeWo CR.SOX10 cell lines as compared to parental cells (Fig. 2C). PI uptake assays using live-cell imaging confirmed significantly increased cell death in A375 *SOX10*-knockout cells treated with TNFα and in MeWo *SOX10*-knockout cells treated with IFNγ (Fig. 2D-E). As a control, we treated cells with IFNα, IFNβ, and transforming growth factor beta (TGFβ) and assessed cell death by flow cytometry. These cytokines had moderate to no effect on cell death in A375 parental and

SOX10-knockout cells, while IFNβ led to similar levels of cell death in both parental and *SOX10*-knockout MeWo cells (Suppl. Fig. 2A, 2B). We also evaluated the effect of other cell death-inducing ligands expressed or secreted by T cells, including tumor necrosis factor-related apoptosis-inducing ligand (TRAIL) and Fas ligand (FasL). We observed increased sensitivity to TRAIL in A375 *SOX10*-knockout cells, but not in 1014 *Sox10*-knockout lines (Suppl. Fig. 2C, 2D).

To understand whether SOX10-deficient cells are more sensitive to cell death in general, we treated cells with staurosporine, an apoptotic inducer (35). We observed no differences in cell death between SOX10-proficient and SOX10-deficient cells at staurosporine concentrations (0.5 μM and 1 μM) used in previous publications (35-37), although *SOX10*-knockout cells were sensitized to cell death at low concentrations (0.1 μM) (Suppl. Fig. 2E, 2F). Overall, these data indicate that TNFα or IFNγ alone are sufficient to promote death in *SOX10*-knockout melanoma cells.

SOX10-deficient cells exhibit unaltered canonical cytokine pathway signaling

Low SOX10 expression has been linked to alterations in cytokine signaling pathways (5,7,38). To assess the effect of SOX10 loss on melanoma cell response to cytokine stimulation, we evaluated signaling downstream of canonical TNFα (NFκB p65 phosphorylation and activation) or IFNγ (STAT1 phosphorylation and activation) receptor activation by Western blot. We did not detect a consistent difference in NFκB p65 phosphorylation between A375 or MeWo parental and *SOX10*-knockout cells following TNFα treatment, although we observed decreased expression of the NFκB p105/p50 subunits in both *SOX10*-knockout models, as well as decreased NFκB p65 expression in MeWo *SOX10*-knockout cells (Fig. 3A, 3B). In both A375 and MeWo cells, we observed similar expression of phosphorylated STAT1 in parental and *SOX10*-knockout cells following IFNγ treatment (Fig. 3C, 3D). Total levels of STAT1 were increased in MeWo *SOX10*-knockout cells; however, we did not detect consistent alterations in its downstream targets, SOCS2 and SOCS3 in either the A375 or MeWo *SOX10*-knockout cells as compared to their parental counterparts (Fig 3C, 3D). In MeWo *SOX10*-knockout cells, we observed decreased levels of the TNF pathway effectors, TRADD and FADD, and the apoptosis effector BCL2; however, these effects were not replicated in A375 cells (Suppl. Fig. 3A, 3B). We also examined the expression of negative regulators of canonical TNFα signaling (OTULIN, A20, and CYLD) and IFNγ signaling (IRF-2 and SHP-2) in parental and *SOX10*-knockout cells treated with cytokine (Suppl. Fig. 3C, 3D) (39,40). While OTULIN and CYLD were decreased in A375 *SOX10*-knockout cells at baseline, there were no consistent differences following TNFα treatment (Suppl. Fig. 3C). There was no change in SHP-2 or IRF-2 expression in MeWo parental versus *SOX10*-knockout cells, untreated or treated with cytokine (Suppl. Fig. 3D). Lastly, we analyzed the expression of TNFα and IFNγ receptors by flow cytometry. While TNFα receptor (TNFR1) was increased only in A375 CR.SOX10 #2.18 cells, *SOX10*-knockout resulted in a moderate increase in A375 cells and a moderate decrease in MeWo cells of IFNγ receptor (IFNGR) (Suppl. Fig. 4A-D). From these data, we conclude that there are no obvious differences in TNFα or IFNγ intracellular signaling pathways following *SOX10*-knockout.

SOX10-knockout cells undergo caspase-dependent cell death

Since we did not detect a SOX10-dependent effect on canonical cytokine-mediated signaling pathways, we investigated whether SOX10 status affects cytokine-mediated cell death. Multiple mechanisms of cell death exist including apoptosis, necroptosis, ferroptosis, and pyroptosis (41). To evaluate the mechanism of cell death induced in *SOX10*-knockout cells by T cell-secreted cytokines, we performed Reverse Phase Protein Array (RPPA) analysis on A375 and MeWo parental and *SOX10*-knockout cells treated with TNFα or IFNγ and identified cell death pathway proteins that were differentially regulated following treatment (Suppl. Table S1). Treatment with either cytokine affected the expression of proteins from multiple cell death pathways (Fig. 4A, 4B, Suppl. Fig. 5A, 5B). Notably, TNFα treatment in A375 *SOX10*-knockout cells and IFNγ treatment in MeWo *SOX10*-knockout cells led to increased caspase cleavage, which is involved in both apoptotic and pyroptotic cell death pathways (Fig. 4A, 4B) (21).

We confirmed that TNFα treatment and IFNγ treatment in A375 and MeWo *SOX10*-knockout cells, respectively, led to cleavage/activation of apoptotic caspases-3 and −8 (Fig. 4C-D, Suppl. Fig. 5C-D). Pre-treatment of cells with the pan-caspase inhibitor Z-VAD-FMK prevented caspase-8 cleavage and cytokine-mediated cell death in A375 and MeWo *SOX10*-knockout cells (Fig. 4E-F, Suppl. Fig. 5E-F). To rule out caspase-independent cell death, we investigated the possible activation of receptor-interacting serine/threonine-protein kinase 1 (RIPK1)-mediated necroptosis. We did not detect RIPK1 activation, assessed by phosphorylation or cleavage following TNFα treatment in A375 CR.SOX10 #4.21 cells (Suppl. Fig. 6A). In addition, treatment with the RIPK1 inhibitor, necrostatin-1, did not prevent TNFα-induced cell death (Suppl. Fig. 6B-C). Thus, we observed that cytokine treatment induced a caspase-dependent, RIPK1-independent cell death response in *SOX10*-knockout cells.

Cytokine-mediated cell death of *SOX10*-knockout cells is associated with markers of pyroptotic cell death

Crosstalk between cell death pathways can occur (21). For example, the apoptosis effectors caspase-3 and caspase-8 can directly cleave gasdermin E (GSDME) to also promote pyroptosis, an inflammatory form of cell death that is capable of amplifying immune responses (21,22,42-44). We determined if cytokine-mediated caspase cleavage is associated with inflammatory cell death in *SOX10*-knockout cells. We observed enhanced cleavage of GSDME in A375 and 1014 *SOX10/Sox10*-knockout cells following TNFα treatment and in MeWo *SOX10*-knockout cells following IFNγ treatment as compared to their parental counterparts (Fig. 5A-B, Suppl. Fig. 7A-C). Pre-treatment with Z-VAD-FMK abolished cytotoxic cytokine-induced GSDME cleavage in A375 and MeWo *SOX10*-knockout cells, suggesting a caspase-dependent effect (Suppl. Fig. 7D-E). In line with effects on cell death, the cytokines TGFβ, IFNα, and IFNβ did not induce cleavage of GSDME in A375 cells, while of these, IFNβ induced GSDME cleavage in both MeWo parental and *SOX10*-knockout cells (Suppl. Fig. 8A-D). Pyroptotic cell death is characterized by pore formation that leads to plasma membrane swelling (45). Using live-cell imaging, we identified membrane swelling in dying *SOX10*-knockout cells treated with TNFα and IFNγ (Fig. 5C). To further examine markers of pyroptotic cell death, we measured exposure of calreticulin

by flow cytometry and release of high mobility group box protein 1 (HMGB1) by Western blotting (22). Upon TNFα or IFNγ cytokine treatment, A375 and MeWo *SOX10*-knockout cells showed increased cell surface levels of calreticulin (Fig. 5D). *SOX10*-knockout led to higher HMGB1 secretion at the resting state, which was further increased in the presence of cytokine treatment in A375 CR.SOX10 #2.18, A375 CR.SOX10 #4.21, and MeWo CR.SOX10 #2.1 knockout cells, although these changes were not statistically significant (Suppl. Fig. 8E-H). Additionally, we investigated the relationship between SOX10 and pyroptosis by analyzing a publicly available database of melanoma patient samples (30,31). We observed that SOX10 mRNA levels are negatively correlated with a pyroptosis gene set (22) in a statistically significant manner (Fig. 5E), suggesting that SOX10 may negatively regulate pyroptosis-related genes. These data demonstrate that *SOX10*-knockout renders cells sensitive to pyroptotic cell death induction by CD8+ T cell-secreted cytokines.

Discussion

The reactivation of neural crest lineage programs is linked to melanoma initiation, and the neural crest lineage transcription factor SOX10 is a key effector in this process (2,46). Notably, SOX10 expression limits the formation of functional anti-tumor immune responses (23,24) and *SOX10*-knockout has been associated with an enrichment in inflammatory signaling pathways (7). In this study, we investigated the role of SOX10 expression in the cellular response to T cell-secreted cytokines. Following SOX10 depletion, we observed increased sensitivity to T cell-mediated killing and an increase in the induction of cell death in response to either IFNγ or TNFα. Conversely, FasL or TRAIL treatment did not have a consistent differential effect on cell death in parental versus *SOX10*-knockout cells. Treatment with IFNγ or TNFα induced caspase-dependent, RIPK1-independent cell death in *SOX10*-knockout cells that was associated with markers of pyroptosis, an inflammatory form of cell death capable of amplifying immune responses (21).

The role of SOX10 in melanoma is complex, as it also positively regulates the expression of MITF, a master regulator of pigmentation genes (47). Melanoma cell lines with low levels of MITF have been shown to exhibit higher inflammatory pathway activity (48), and MITF modulates anti-tumor immune responses (49). Downregulation of MITF is critical for IFNγ-mediated cytotoxicity in melanoma cells and is associated with response to immune checkpoint blockade in patients (50,51). Thus, it is possible that MITF loss may contribute to the cytokine-mediated cell death observed in our SOX10-deficient cells. Heterogeneity in MITF expression and cell state in our parental cell lines may also explain why we see differences in sensitivity to TNFα versus IFNγ treatment following *SOX10*-knockout; while A375 cells are considered MITF-low and ‘neural-crest-like’, MeWo cells express high levels of both MITF and SOX10, suggesting they have a more ‘melanocytic’ or ‘proliferative’ cell state (5,52). Given that tumors are composed of cells in various cell states, heterogeneity could affect how SOX10-deficient cells respond to T cell killing. SOX10 and MITF loss also reduces the transcription of melanocytic antigens (53,54), which are common targets for antigen-specific T cells. While T cells are activated toward antigen for an *in vitro* T cell killing assay, it is possible that the loss of tumor-specific antigens limits the overall effect of direct and indirect T cell killing in patient tumors. Thus, exploiting the vulnerability

of SOX10-deficient cells in tumors to T cell killing may require the induction of immune responses against non-melanocytic neoantigens.

The loss of SOX10 has been observed in tumor cells that have acquired metastatic capabilities or become resistant to targeted therapy (5-8). Our findings suggest that these invasive, therapy-resistant SOX10-deficient cells are still vulnerable to T cell killing, which is in line with other studies that demonstrate SOX10 regulation of tumor growth in a T cell-dependent manner (23,24). Thus, we hypothesize that factors independent of T cell killing may contribute to the persistence of SOX10-deficient cells in patient tumors, including an immunosuppressed tumor niche or immune cell exclusion. The loss of SOX10 differentially affects immune checkpoint protein expression (23,55), but the effect on T cell activation is not known. Alterations in the secretome of SOX10-deficient cells may lead to the recruitment and differentiation of pro-tumorigenic immune cell populations (56). Blocking inhibitory checkpoints or cytokines could be effective in promoting T cell killing of SOX10-deficient melanoma cells. Additionally, the production of stromal components by tumor cells or cancer-associated fibroblasts may limit T cell infiltration into the tumor (57-59). Therefore, developing therapeutic options that increase the interaction between T cells and tumor cells will be beneficial.

SOX10 was recently shown to positively regulate the expression of pyroptosis-related genes and gasdermin-D cleavage in a non-oncogenic cell model (60). Here, we observed that cytokine-mediated cell death of *SOX10*-deficient melanoma cells was associated with markers of GSDME-mediated pyroptosis. We cannot rule out that other forms of cell death, particularly apoptosis, may also be occurring in our *SOX10*-knockout cells. However, pyroptotic cell death is of particular interest given that it promotes the release of multiple inflammatory and immune stimulatory factors (21). Secreted HMGB1 elicits pro-inflammatory effects on the immune system and is thought to be critical for cell death to be immunogenic (61,62). Cell surface exposure of calreticulin promotes the phagocytic clearance and engulfment of tumor cells by antigen presenting cells, which also promotes immunogenicity (63,64). Importantly, this mode of cell death can promote immune cell recruitment and augment immune responses in cancer. Thus, it is possible that the requirement for SOX10 in melanomagenesis may be partially dependent on its ability to protect malignant cells from T cell killing and cytokine secretion. Our findings suggest that SOX10-deficient cells are not only sensitive to T cell-mediated killing, but the resulting cell death may further propagate anti-tumor immune responses. Future studies should focus on finding therapies that enhance immunogenic cell death and immune cell recruitment in this subpopulation of tumor cells.

Supplementary Material

Refer to Web version on PubMed Central for supplementary material.

Acknowledgments:

We are grateful to Dr. Meenhard Herlyn (The Wistar Institute), Dr. Lionel Larue (Institut Curie), Dr. Barbara Bedogni (University of Miami Health System), and Dr. Marcus Bosenberg (Yale School of Medicine) for generously providing cell lines. This work is supported by grants from National Institutes of Health (NIH)/National

Cancer Institute (NCI) R01s CA196278 and CA182635 and project 4 of P01 CA114046-11A1 to A.E. Aplin, by F99 CA245552 to S.R. Rosenbaum, by T32 CA236736 (PIs are Drs Bruno Calabretta and Andrew Aplin) and by T32 GM100836 and T32 GM144302 (PI is Dr. Jeffrey Benovic). Additionally, the study was supported by an award from the Dr. Miriam and Sheldon G. Adelson Medical Research Foundation to A.E. Aplin and grants from the American Cancer Society (130042-IRG-16-244-10-IRG to Dr. Andrew Chapman), Melanoma Research Foundation, and Legacy of Hope Merit of Award to C. Capparelli. S. Caksa is funded by a Medical Student Award from the Melanoma Research Foundation. The Sidney Kimmel Cancer Center Flow Cytometry, Meta-Omics, Translational Pathology, and Laboratory Animal core facilities are supported by a National Cancer Center Support Grant (P30 CA056036). The RPPA studies were performed at the Functional Proteomics Core Facility at The University of Texas MD Anderson Cancer Center, which is supported by a NIH/NCI Cancer Center Support Grant (P30 CA16672).

References

1. Simões-Costa M, and Bronner ME. Establishing neural crest identity: a gene regulatory recipe. Development 2015;142:242–257 [PubMed: 25564621]
2. Shakhova O, Zingg D, Schaefer SM, Hari L, Civenni G, Blunschi J, et al. Sox10 promotes the formation and maintenance of giant congenital naevi and melanoma. Nat Cell Biol 2012;14:882–890 [PubMed: 22772081]
3. Cronin JC, Watkins-Chow DE, Incao A, Hasskamp JH, Schönewolf N, Aoude LG, et al. SOX10 ablation arrests cell cycle, induces senescence, and suppresses melanomagenesis. Cancer Res 2013;73:5709–5718 [PubMed: 23913827]
4. Dunn GP, Bruce AT, Ikeda H, Old LJ, and Schreiber RD. Cancer immunoediting: from immunosurveillance to tumor escape. Nat Immunol 2002;3:991–998 [PubMed: 12407406]
5. Wouters J, Kalender-Atak Z, Minnoye L, Spanier KI, De Waegeneer M, Bravo González-Blas C, et al. Robust gene expression programs underlie recurrent cell states and phenotype switching in melanoma. Nat Cell Biol 2020;22:986–998 [PubMed: 32753671]
6. Rambow F, Rogiers A, Marin-Bejar O, Aibar S, Femel J, Dewaele M, et al. Toward minimal residual disease-directed therapy in melanoma. Cell 2018;174:843–855.e819 [PubMed: 30017245]
7. Capparelli C, Purwin TJ, Glasheen M, Caksa S, Tiago M, Wilski N, et al. Targeting SOX10-deficient cells to reduce the dormant-invasive phenotype state in melanoma. Nat Commun 2022;13:1381 [PubMed: 35296667]
8. Sun C, Wang L, Huang S, Heynen GJJE, Prahallad A, Robert C, et al. Reversible and adaptive resistance to BRAF(V600E) inhibition in melanoma. Nature 2014;508:118–122 [PubMed: 24670642]
9. Glasheen MQ, Caksa S, Young AG, Wilski NA, Ott CA, Chervoneva I, et al. Targeting up-regulated cIAP2 in SOX10-deficient drug tolerant melanoma. Mol Cancer Ther 2023;Online ahead of print.
10. Martínez-Lostao L, Anel A, and Pardo J. How do cytotoxic lymphocytes kill cancer cells? Clin Cancer Res 2015;21:5047–5056 [PubMed: 26567364]
11. Chawla-Sarkar M, Lindner DJ, Liu YF, Williams BR, Sen GC, Silverman RH, et al. Apoptosis and interferons: role of interferon-stimulated genes as mediators of apoptosis. Apoptosis 2003;8:237–249 [PubMed: 12766484]
12. Bhat P, Leggatt G, Waterhouse N, and Frazer IH. Interferon-γ derived from cytotoxic lymphocytes directly enhances their motility and cytotoxicity. Cell Death Dis 2017;8:e2836 [PubMed: 28569770]
13. Vredevoogd DW, Kuilman T, Ligtenberg MA, Boshuizen J, Stecker KE, de Bruijn B, et al. Augmenting immunotherapy impact by lowering tumor TNF cytotoxicity threshold. Cell 2019;178:585–599.e515 [PubMed: 31303383]
14. Kearney CJ, Vervoort SJ, Hogg SJ, Ramsbottom KM, Freeman AJ, Lalaoui N, et al. Tumor immune evasion arises through loss of TNF sensitivity. Sci Immunol 2018;3:eaar3451 [PubMed: 29776993]
15. Lawson KA, Sousa CM, Zhang X, Kim E, Akthar R, Caumanns JJ, et al. Functional genomic landscape of cancer-intrinsic evasion of killing by T cells. Nature 2020;586:120–126 [PubMed: 32968282]

16. Manguso RT, Pope HW, Zimmer MD, Brown FD, Yates KB, Miller BC, et al. In vivo CRISPR screening identifies Ptpn2 as a cancer immunotherapy target. Nature 2017;547:413–418 [PubMed: 28723893]
17. Matsushita H, Hosoi A, Ueha S, Abe J, Fujieda N, Tomura M, et al. Cytotoxic T lymphocytes block tumor growth both by lytic activity and IFNγ-dependent cell-cycle arrest. Cancer Immunol Res 2015;3:26–36 [PubMed: 25127875]
18. Sucker A, Zhao F, Pieper N, Heeke C, Maltaner R, Stadtler N, et al. Acquired IFNγ resistance impairs anti-tumor immunity and gives rise to T-cell-resistant melanoma lesions. Nat Commun 2017;8:15440 [PubMed: 28561041]
19. Larkin J, Chiarion-Sileni V, Gonzalez R, Grob JJ, Rutkowski P, Lao CD, et al. Five-year survival with combined nivolumab and ipilimumab in advanced melanoma. N Engl J Med 2019;381:1535–1546 [PubMed: 31562797]
20. Tumeh PC, Harview CL, Yearley JH, Shintaku IP, Taylor EJM, Robert L, et al. PD-1 blockade induces responses by inhibiting adaptive immune resistance. Nature 2014;515:568–571 [PubMed: 25428505]
21. Rosenbaum SR, Wilski NA, and Aplin AE. Fueling the fire: inflammatory forms of cell death and implications for cancer immunotherapy. Cancer Discov 2021;11:266–281 [PubMed: 33451983]
22. Erkes DA, Cai W, Sanchez IM, Purwin TJ, Rogers C, Field CO, et al. Mutant BRAF and MEK inhibitors regulate the tumor immune microenvironment via pyroptosis. Cancer Discov 2020;10:254–269 [PubMed: 31796433]
23. Rosenbaum SR, Tiago M, Caksa S, Capparelli C, Purwin TJ, Kumar G, et al. SOX10 requirement for melanoma tumor growth is due, in part, to immune-mediated effects. Cell Rep 2021;37:110085 [PubMed: 34879275]
24. Abou-Hamad J, Hodgins JJ, de Souza CT, Garland B, Labrèche C, Marotel M, Gibson C, Delisle S, Pascoal J, Auer RC, Ardolino M, Sabourin LA CEACAM1 is a direct SOX10 target and inhibits melanoma immune infiltration and stemness. iScience 2022;25:105524 [PubMed: 36437876]
25. Tibes R, Qiu Y, Lu Y, Hennessy B, Andreeff M, Mills GB, et al. Reverse phase protein array: validation of a novel proteomic technology and utility for analysis of primary leukemia specimens and hematopoietic stem cells. Mol Cancer Ther 2006;5:2512–2521 [PubMed: 17041095]
26. The Gene Ontology Consortium, Ashburner M, Ball CA, Blake JA, Botstein D, Butler H, et al. Gene ontology: tool for the unification of biology. Nat Genet 2000;25:25–29 [PubMed: 10802651]
27. The Gene Ontology Consortium. The Gene Ontology Resource: 20 years and still GOing strong. Nucleic Acids Res 2019;47:D330–D338 [PubMed: 30395331]
28. Kanehisa M, and Goto S. KEGG: kyoto encyclopedia of genes and genomes. Nucleic Acids Res 2000;28:27–30 [PubMed: 10592173]
29. Galluzzi L, Vitale I, Aaronson SA, Abrams JM, Adam D, Agostinis P, et al. Molecular mechanisms of cell death: recommendations of the Nomenclature Committee on Cell Death 2018. Cell Death Differ 2018;25:486–541 [PubMed: 29362479]
30. Cerami E, Gao J, Dogrusoz U, Gross BE, Sumer SO, Aksoy BA, et al. The cBio cancer genomics portal: an open platform for exploring multidimensional cancer genomics data. Cancer Discov 2012;2:401–404 [PubMed: 22588877]
31. Gao J, Aksoy BA, Dogrusoz U, Dresdner G, Gross B, Sumer SO, et al. Integrative analysis of complex cancer genomics and clinical profiles using the cBioPortal. Sci Signal 2013;6:pl1
32. Petit V, Raymond J, Alberti C, Pouteaux M, Gallagher SJ, Nguyen MQ, et al. C57BL/6 congenic mouse NRASQ61K melanoma cell lines are highly sensitive to the combination of Mek and Akt inhibitors in vitro and in vivo. Pigment Cell Melanoma Res 2019;32:829–841 [PubMed: 31251472]
33. Overwijk WW, Tsung A, Irvine KR, Parkhurst MR, Goletz TJ, Tsung K, et al. gp100/pmel 17 Is a murine tumor rejection antigen: induction of “self”-reactive, tumoricidal T cells using high-affinity, altered peptide ligand. J Exp Med 1998;188:277–286 [PubMed: 9670040]
34. Braumüller H, Wieder T, Brenner E, Aßmann S, Hahn M, Alkhaled M, et al. T-helper-1-cell cytokines drive cancer into senescence. Nature 2013;494:361–365 [PubMed: 23376950]

35. Zhang XD, Gillespie SK, and Hersey P. Staurosporine induces apoptosis of melanoma by both caspase-dependent and -independent apoptotic pathways. Mol Cancer Ther 2004;3:187–197 [PubMed: 14985459]
36. Antonsson A, and Persson JL. Induction of apoptosis by staurosporine involves the inhibition of expression of the major cell cycle proteins at the G2/M checkpoint accompanied by alterations in Erk and Akt kinase activities. Anticancer Res 2009;29:2893–2898 [PubMed: 19661292]
37. Dunai ZA, Imre G, Barna G, Korcsmaros T, Petak I, Bauer PI, et al. Staurosporine induces necroptotic cell death under caspase-compromised conditions in U937 cells. PLoS One 2012;7:e41945 [PubMed: 22860037]
38. Laurette P, Coassolo S, Davidson G, Michel I, Gambi G, Yao W, et al. Chromatin remodellers Brg1 and Bptf are required for normal gene expression and progression of oncogenic Braf-driven mouse melanoma. Cell Death Differ 2020;27:29–43 [PubMed: 31065107]
39. Webster JD, and Vucic D. The Balance of TNF Mediated Pathways Regulates Inflammatory Cell Death Signaling in Healthy and Diseased Tissues. Front Cell Dev Biol 2020;8:365 [PubMed: 32671059]
40. Schroder K, Hertzog PJ, Ravasi T, and Hume DA. Interferon-gamma: an overview of signals, mechanisms and functions. J Leukoc Biol 2004;75:163–189 [PubMed: 14525967]
41. Kist M, and Vucic D. Cell death pathways: intricate connections and disease implications. EMBO Journal 2021;40:e106700 [PubMed: 33439509]
42. Rogers C, Erkes DA, Nardone A, Aplin AE, Fernandes-Alnemri T, and Alnemri ES. Gasdermin pores permeabilize mitochondria to augment caspase-3 activation during apoptosis and inflammasome activation. Nat Commun 2019;10:1689 [PubMed: 30976076]
43. Wang Y, Gao W, Shi X, Ding J, Liu W, He H, et al. Chemotherapy drugs induce pyroptosis through caspase-3 cleavage of a gasdermin. Nature 2017;547:99–103 [PubMed: 28459430]
44. Aizawa E, Karasawa T, Watanabe S, Komada T, Kimura H, Kamata R, et al. GSDME-Dependent Incomplete Pyroptosis Permits Selective IL-1α Release under Caspase-1 Inhibition. iScience 2020;23:101070 [PubMed: 32361594]
45. Rogers C, Fernandes-Alnemri T, Mayes L, Alnemri D, Cingolani G, and Alnemri ES. Cleavage of DFNA5 by caspase-3 during apoptosis mediates progression to secondary necrotic/pyroptotic cell death. Nat Commun 2017;8:14128 [PubMed: 28045099]
46. Kaufman CK, Mosimann C, Fan ZP, Yang S, Thomas AJ, Ablain J, et al. A zebrafish melanoma model reveals emergence of neural crest identity during melanoma initiation. Science 2016;351:aad2197 [PubMed: 26823433]
47. Verastegui C, Bille K, Ortonne JP, and Ballotti R. Regulation of the microphthalmia-associated transcription factor gene by the Waardenburg syndrome type 4 gene, SOX10. J Biol Chem 2000;275:30757–30760 [PubMed: 10938265]
48. Riesenberg S, Groetchen A, Siddaway R, Bald T, Reinhardt J, Smorra D, et al. MITF and c-Jun antagonism interconnects melanoma dedifferentiation with pro-inflammatory cytokine responsiveness and myeloid cell recruitment. Nat Commun 2015;6:8755 [PubMed: 26530832]
49. Sánchez-del-Campo L, Martí-Díaz R, Montenegro MF, González-Guerrero R, Hernández-Caselles T, Martínez-Barba E, et al. MITF induces escape from innate immunity in melanoma. J Exp Clin Cancer Res 2021;40:117 [PubMed: 33789714]
50. Kenski JCN, Huang X, Vredevoogd DW, de Bruijn B, Traets JJH, Ibáñez-Molero S, et al. An adverse tumor-protective effect of IDO1 inhibition. Cell Rep Med 2023;4:100941 [PubMed: 36812891]
51. Kim YJ, Sheu KM, Tsoi J, Abril-Rodriguez G, Medina E, Grasso CS, et al. Melanoma dedifferentiation induced by IFN-γ epigenetic remodeling in response to anti-PD-1 therapy. J Clin Invest 2021;131
52. Vlčková K, Vachtenheim J, Réda J, Horák P, and Ondrušová L. Inducibly decreased MITF levels do not affect proliferation and phenotype switching but reduce differentiation of melanoma cells. J Cell Mol Med 2018;22:2240–2251 [PubMed: 29369499]
53. Landsberg J, Kohlmeyer J, Renn M, Bald T, Rogava M, Cron M, et al. Melanomas resist T-cell therapy through inflammation-induced reversible dedifferentiation. Nature 2012;490:412–416 [PubMed: 23051752]

54. Mehta A, Kim YJ, Robert L, Tsoi J, Comin-Anduix B, Berent-Maoz B, et al. Immunotherapy resistance by inflammation-induced dedifferentiation. Cancer Discov 2018;8:935–943 [PubMed: 29899062]

55. Yokoyama S, Takahashi A, Kikuchi R, Nishibu S, Lo JA, Hejna M, et al. SOX10 Regulates Melanoma Immunogenicity through an IRF4-IRF1 Axis. Cancer Res 2021;81:6131–6141 [PubMed: 34728538]

56. Kohli K, Pillarisetty VG, and Kim TS. Key chemokines direct migration of immune cells in solid tumors. Cancer Gene Ther 2022;29:10–21 [PubMed: 33603130]

57. Salmon H, Franciszkiewicz K, Damotte D, Dieu-Nosjean MC, Validire P, Trautmann A, et al. Matrix architecture defines the preferential localization and migration of T cells into the stroma of human lung tumors. J Clin Invest 2012;122:899–910 [PubMed: 22293174]

58. Jenkins L, Jungwirth U, Avgustinova A, Iravani M, Mills A, Haider S, et al. Cancer-Associated Fibroblasts Suppress CD8+ T-cell Infiltration and Confer Resistance to Immune-Checkpoint Blockade. Cancer Res 2022;82:2904–2917 [PubMed: 35749591]

59. Sun X, Wu B, Chiang HC, Deng H, Zhang X, Xiong W, et al. Tumour DDR1 promotes collagen fibre alignment to instigate immune exclusion. Nature 2021;599:673–678 [PubMed: 34732895]

60. Xu X, Zhang DD, Kong P, Gao YK, Huang XF, Song Y, et al. Sox10 escalates vascular inflammation by mediating vascular smooth muscle cell transdifferentiation and pyroptosis in neointimal hyperplasia. Cell Rep 2023;42:112869 [PubMed: 37481722]

61. Green DR, Ferguson T, Zitvogel L, and Kroemer G. Immunogenic and tolerogenic cell death. Nat Rev Immunol 2009;9:353–363 [PubMed: 19365408]

62. Scaffidi P, Misteli T, and Bianchi ME. Release of chromatin protein HMGB1 by necrotic cells triggers inflammation. Nature 2002;418:191–195 [PubMed: 12110890]

63. Feng M, Marjon KD, Zhu F, Weissman-Tsukamoto R, Levett A, Sullivan K, et al. Programmed cell removal by calreticulin in tissue homeostasis and cancer. Nat Commun 2018;9:3194–3194 [PubMed: 30097573]

64. Obeid M, Tesniere A, Ghiringhelli F, Fimia GM, Apetoh L, Perfettini JL, et al. Calreticulin exposure dictates the immunogenicity of cancer cell death. Nat Med 2007;13:54–61 [PubMed: 17187072]

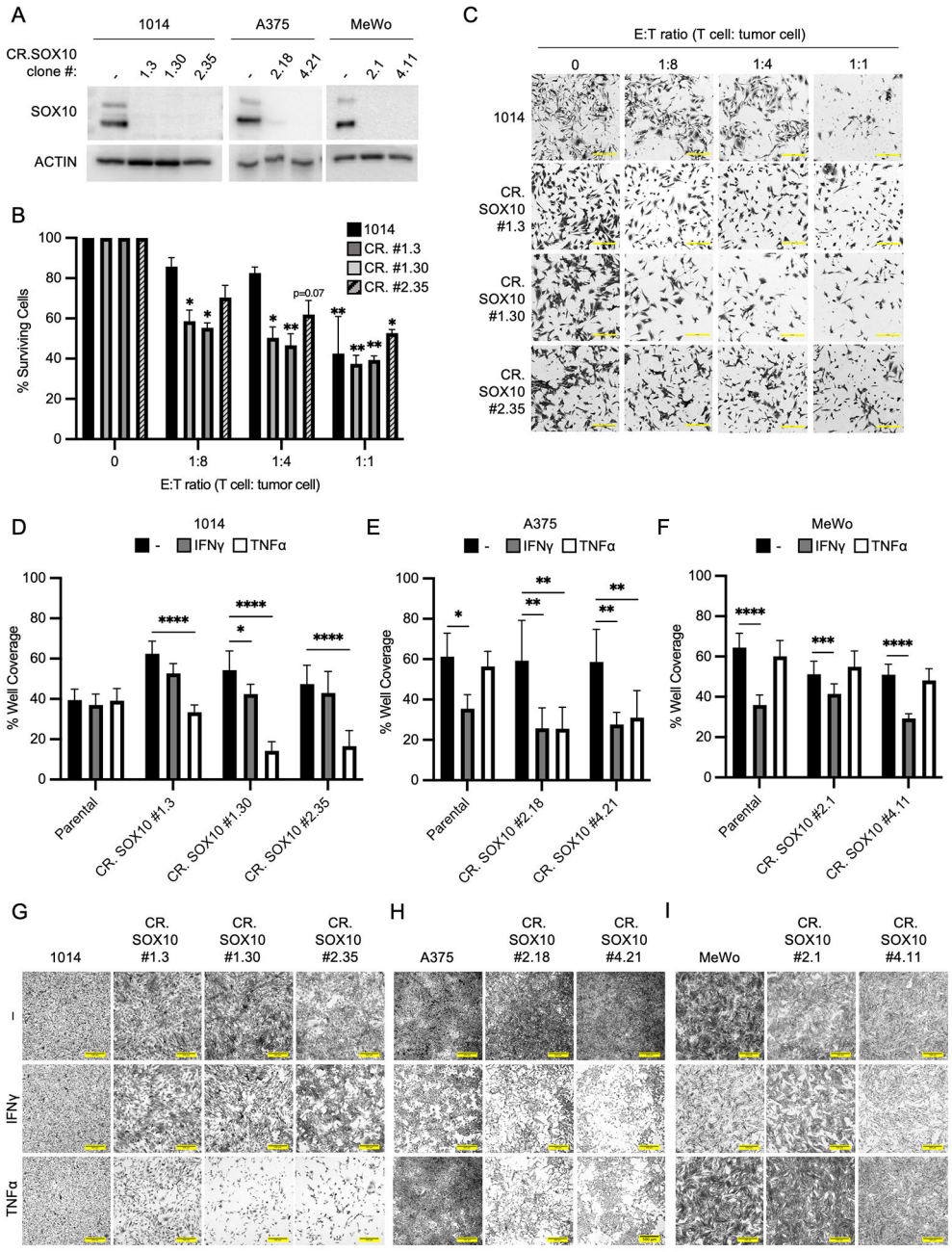

Figure 1: Cytotoxic T cell-secreted cytokines reduce the growth of *SOX10/Sox10*-knockout cells

A) CRISPR/Cas9 knockout of *Sox10/SOX10* in 1014, A375, and MeWo cells was verified by Western blot. B) 1014 parental or *Sox10*-knockout cells were peptide-pulsed for 3 hours and incubated with Pmel-1 T cells for 48 hours. Cancer cells were washed and stained by crystal violet. Wells were imaged, well coverage was quantified on ImageJ, and % surviving cells was graphed. C) Images representative of three independent experiments from (B). Scale bars represent 250 μm D) 1014 parental or *Sox10*-knockout cells were treated with 100 ng/mL IFNγ or 50 ng/mL TNFα for 72 hours. Cancer cells were washed and stained with crystal violet. Wells were imaged, and percent well coverage was quantified on ImageJ.

E) As in D, for A375 parental or *SOX10*-knockout cells. F) As in D, for MeWo parental or *SOX10*-knockout cells. G) Images representative of three independent experiments from (D). Scale bars represent 500 μm. H) As in G, for data shown in (E). I) As in G, for data shown in (F). All data are representative of three independent experiments. Bar graphs show mean + SD. *p<0.05, **p<0.01, ***p<0.001, ****p<0.0001.

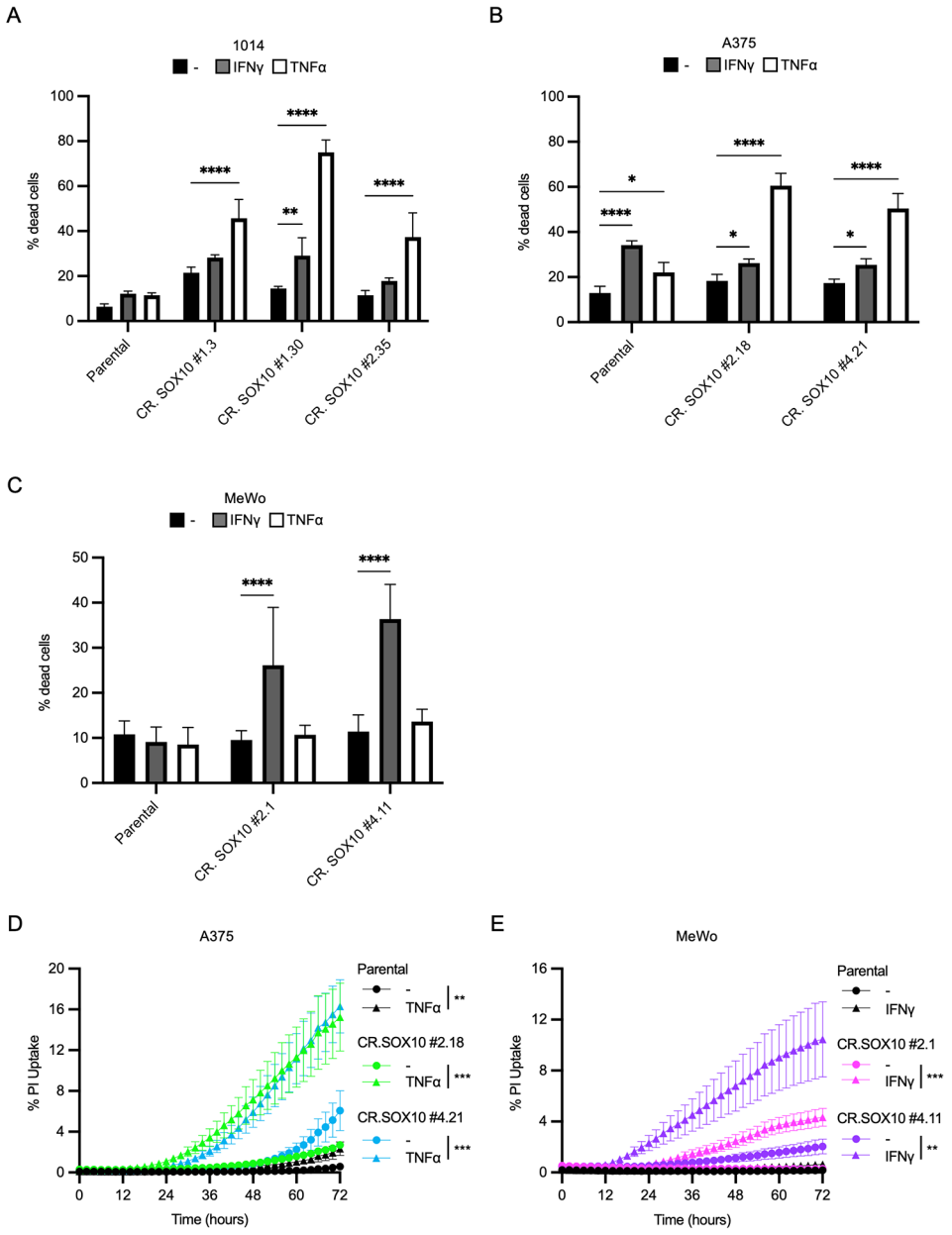

Figure 2: *SOX10/Sox10*-knockout sensitizes melanoma cells to cytokine-mediated cell death

A) 1014 parental or *Sox10*-knockout cells were treated with 100 ng/mL IFNγ or 50 ng/mL TNFα for 72 hours. Cell death was evaluated by Annexin V, propidium iodide (PI), and dual Annexin V/PI staining by flow cytometry. B) As in A, for A375 parental or *SOX10*-knockout cells. C) As in A, for MeWo parental or *SOX10*-knockout cells. D) A375 parental or *SOX10*-knockout cells were treated with 50 ng/mL TNFα for 72 hours. PI was added to a final concentration of 0.5 μM at the time of treatment, and phase contrast and RFP images were taken every 2 hours at 10x using live-cell imaging. Percent PI uptake at each time point was calculated using the formula (percent red confluence/percent phase confluence) x 100. E) As in D, for MeWo parental or *SOX10*-knockout cells treated with 100 ng/mL IFNγ. All data are representative of three independent experiments, except in (C) and (E) where six

and four independent experiments were conducted, respectively. Bar graphs show mean + SD. Line graphs show mean ± SEM. *p<0.05, **p<0.01, ***p<0.001, ****p<0.0001.

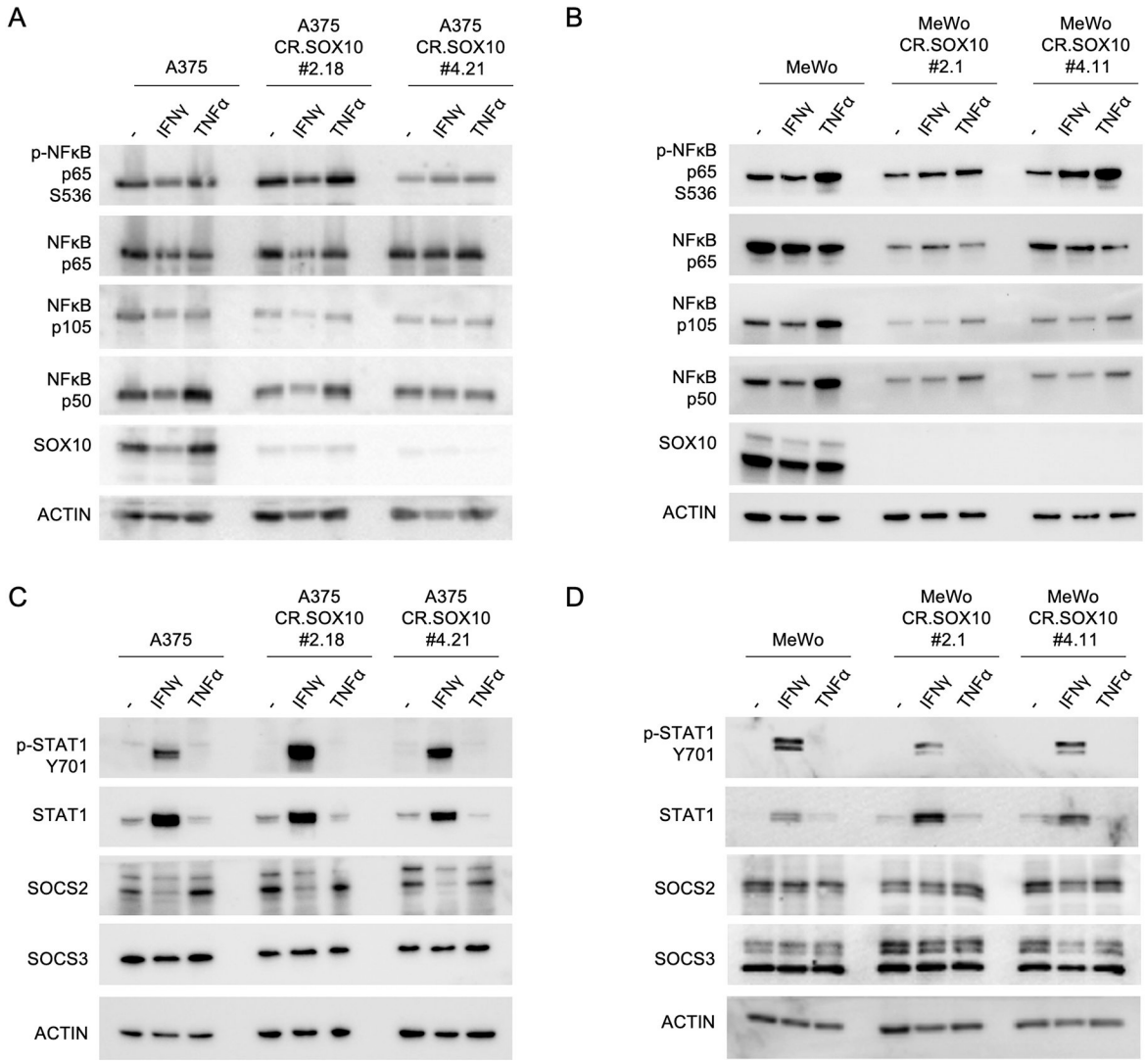

Figure 3: Analysis of canonical cytokine signaling pathways in SOX10-deficient cells

A) A375 parental or *SOX10*-knockout cells were treated with 100 ng/mL IFNγ or 50 ng/mL TNFα for 72 hours. Cells were lysed and lysates were probed for canonical signaling downstream of TNFα receptor activation by Western blot. B) As in A, for MeWo parental or *SOX10*-knockout cells. C) A375 parental or *SOX10*-knockout cells were treated with 100 ng/mL IFNγ or 50 ng/mL TNFα for 72 hours. Cells were lysed and lysates were probed for canonical signaling downstream of IFNγ receptor activation by Western blot. D) As in C, for MeWo parental or *SOX10*-knockout cells. All data are representative of three independent experiments.

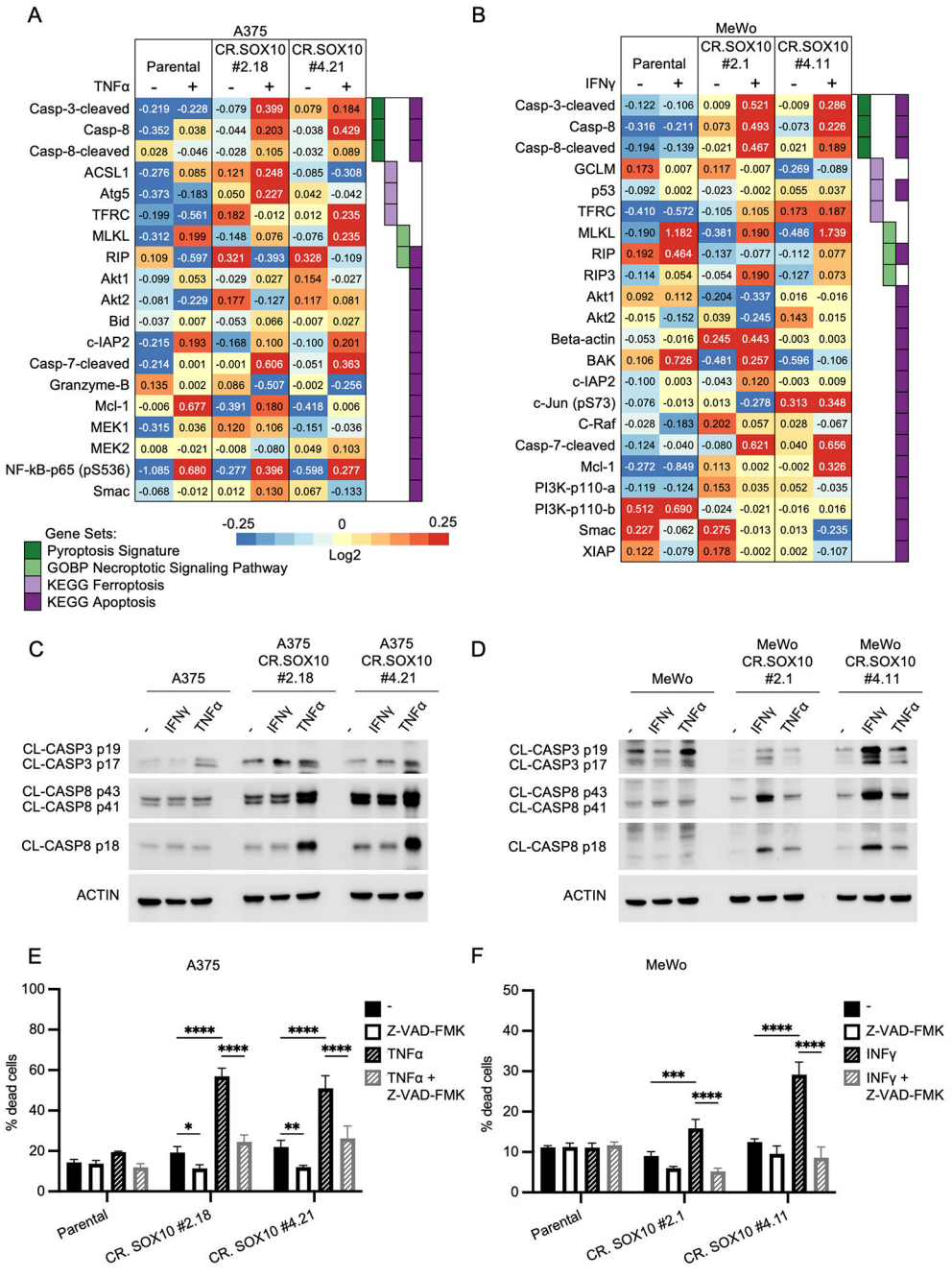

Figure 4: Cytokine-induced cell death in *SOX10*-knockout cells is caspase-dependent

A) A375 parental or *SOX10*-knockout cells were treated with 50 ng/mL TNFα for 72 hours and lysates were collected for RPPA analysis. A heat map displays median-centered, log2-transformed group average expression data for cell death pathway proteins with a p-value < 0.05 for any comparison. B) As in A, except MeWo parental or *SOX10*-knockout cells were treated with 100 ng/mL IFNγ for 72 hours. C) A375 parental or *SOX10*-knockout cells were treated with 100 ng/mL IFNγ or 50 ng/mL TNFα for 72 hours. Cells were lysed and lysates were probed for cleavage of caspases by Western blot. D) As in C, for MeWo parental or *SOX10*-knockout cells. E) A375 parental or *SOX10*-knockout cells were

pre-treated with 50 μM of the pan-caspase inhibitor Z-VAD-FMK for 30 minutes prior to treatment with 50 ng/mL TNFα for 72 hours. Cell death was then evaluated by Annexin V, propidium iodide (PI), and dual Annexin V/PI staining by flow cytometry. F) As in E, except MeWo parental or *SOX10*-knockout cells were treated with 100 ng/mL IFNγ after 50 μM Z-VAD-FMK pre-treatment. All data are representative of three independent experiments. Bar graphs show mean + SD. *p<0.05, **p<0.01, ***p<0.001, ****p<0.0001.

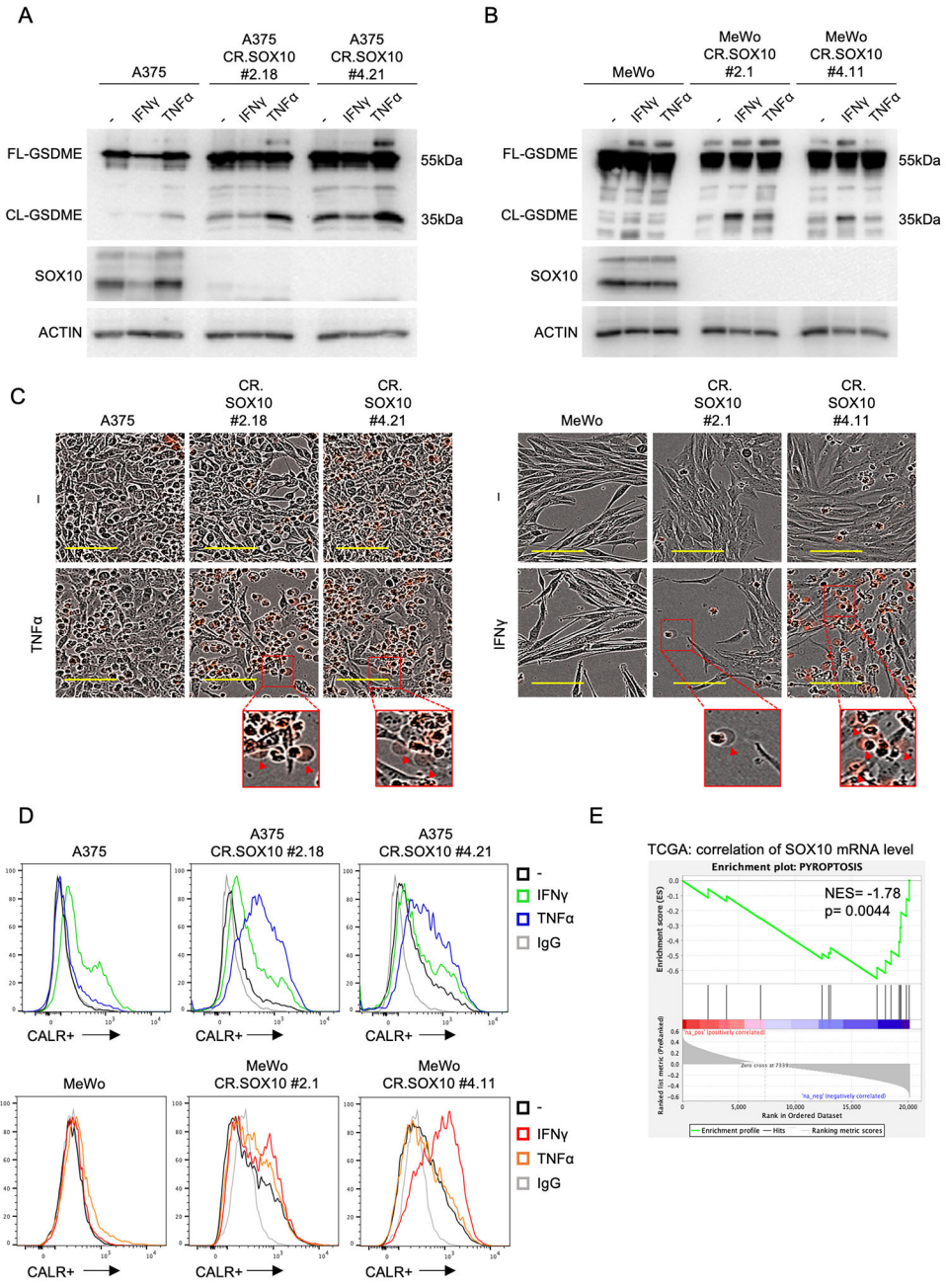

Figure 5: Cytokine-induced cell death in *SOX10*-knockout cells is associated with markers of pyroptosis

A) A375 parental or *SOX10*-knockout cells were treated with 100 ng/mL IFNγ or 50 ng/mL TNFα for 72 hours. Cells were lysed and lysates were probed for cleavage of GSDME by Western blot. Data are representative of three independent experiments. B) As in A, for MeWo parental or *SOX10*-knockout cells. C) A375 or MeWo, parental or *SOX10*-knockout cells were treated with 50 ng/mL TNFα or 100 ng/mL IFNγ, respectively. 0.5 μM PI was added at the time of treatment, and phase contrast and RFP images were taken after 72 hours at 10x using live-cell imaging. Examples of plasma membrane swelling are indicated with red arrows in inset images. Scale bars represent 100 μm. Images are representative of

three independent experiments. D) A375 or MeWo, parental or *SOX10*-knockout cells, were treated with 100 ng/mL IFNγ or 50 ng/mL TNFα for 72 hours, and calreticulin expression was evaluated by flow cytometry staining. Data are representative of three independent experiments. E) A TCGA melanoma dataset was evaluated for the correlation between SOX10 mRNA levels and a pyroptosis gene signature.